Original Article | Neuroimaging and Head & Neck

eISSN 2005-8330
https://doi.org/10.3348/kjr.2022.0980
Korean J Radiol 2023;24(5):444-453

Korean Journal of Radiology
KJR

Assessment of Meningeal Lymphatics in the Parasagittal Dural Space: A Prospective Feasibility Study Using Dynamic Contrast-Enhanced Magnetic Resonance Imaging

Bio Joo, Mina Park, Sung Jun Ahn, Sang Hyun Suh

Department of Radiology, Gangnam Severance Hospital, Yonsei University College of Medicine, Seoul, Korea

Objective: Meningeal lymphatic vessels are predominantly located in the parasagittal dural space (PSD); these vessels drain interstitial fluids out of the brain and contribute to the glymphatic system. We aimed to investigate the ability of dynamic contrast-enhanced magnetic resonance imaging (DCE-MRI) in assessing the dynamic changes in the meningeal lymphatic vessels in PSD.

Materials and Methods: Eighteen participants (26–71 years; male:female, 10:8), without neurological or psychiatric diseases, were prospectively enrolled and underwent DCE-MRI. Three regions of interests (ROIs) were placed on the PSD, superior sagittal sinus (SSS), and cortical vein. Early and delayed enhancement patterns and six kinetic curve-derived parameters were obtained and compared between the three ROIs. Moreover, the participants were grouped into the young (< 65 years; n = 9) or older (≥ 65 years; n = 9) groups. Enhancement patterns and kinetic curve-derived parameters in the PSD were compared between the two groups.

Results: The PSD showed different enhancement patterns than the SSS and cortical veins (P < 0.001 and P < 0.001, respectively) in the early and delayed phases. The PSD showed slow early enhancement and a delayed wash-out pattern. The six kinetic curve-derived parameters of PSD was significantly different than that of the SSS and cortical vein. The PSD wash-out rate of older participants was significantly lower (median, 0.09; interquartile range [IQR], 0.01–0.15) than that of younger participants (median, 0.32; IQR, 0.07–0.45) (P = 0.040).

Conclusion: This study shows that the dynamic changes of meningeal lymphatic vessels in PSD can be assessed with DCE-MRI, and the results are different from those of the venous structures. Our finding that delayed wash-out was more pronounced in the PSD of older participants suggests that aging may disturb the meningeal lymphatic drainage.

Keywords: Aging; Central nervous system; Glymphatic system; Meningeal lymphatic system; Magnetic resonance imaging

INTRODUCTION

For several decades, the central nervous system (CNS) has been considered an immune-privileged organ as it has not been considered part of the lymphatic system [1,2]. However, the existence of meningeal lymphatic vessels was first described in animal studies by Aspelund et al. [3] and Louveau et al. in 2015 [4], and its presence was further evidenced by human studies [5-8]. The meningeal lymphatic vessels are found alongside the major venous sinus, cranial nerves, and arteries, and the meningeal lymphatic vessels drain cerebrospinal fluid (CSF) and interstitial fluid (ISF) from the CNS into the extracranial cervical lymph nodes [3,4,9]. In addition to its involvement in clearing brain waste, regulating CSF, and maintaining brain homeostasis, meningeal lymphatics may be an important drainage route for CSF/ISF of the brain, and it is considered to be closely related to the glymphatic system, which is a glia-dependent system of perivascular channels [3,4,10].

Several human studies have demonstrated the presence of meningeal lymphatics in the parasagittal dural space

Received: December 12, 2022 **Revised:** February 14, 2023
Accepted: February 27, 2023
Corresponding author: Mina Park, MD, PhD, Department of Radiology, Gangnam Severance Hospital, Yonsei University College of Medicine, 211 Eonju-ro, Gangnam-gu, Seoul 06273, Korea.
• E-mail: to.minapark@yuhs.ac

Korean Journal of Radiology
KJR

(PSD) around the superior sagittal sinus (SSS) using in vivo magnetic resonance imaging (MRI) with intravenous or intrathecal gadolinium contrast enhancement [6,7]. One study showed that meningeal lymphatic drainage in the PSD was impaired in the aging human brain; the study used multiple time point fluid-attenuated inversion recovery imaging (FLAIR) acquisitions following intrathecal administration of a gadolinium contrast agent [11].

Intrathecal injection of a gadolinium contrast agent may enable direct visualization of meningeal lymphatic function [11-13]. Off-label intrathecal injection of a gadolinium contrast agent has been reported to be safe when using an appropriate low-dose injection; however, non-serious adverse events, such as headache, nausea, and dizziness, have been reported [14]. Furthermore, intrathecal administration of gadolinium contrast agents on an outpatient basis is not easily applicable, as it requires multiple time point acquisitions of up to 48 hours [14], which may limit wider clinical application and research potential. Therefore, less invasive and rapid methods of dynamic assessment and quantification of meningeal lymphatic drainage in humans are needed for widespread clinical application.

However, few studies have investigated the dynamic aspect of meningeal lymphatic vessels using intravenous administration of a gadolinium contrast agent [15,16]. One previous study applied dynamic contrast-enhanced MRI (DCE-MRI) to compare meningeal lymphatic flow in patients with idiopathic Parkinson's disease and suggested DCE-MRI as a promising imaging biomarker for quantifying meningeal lymphatic flow [16]. However, further research is required to determine the usefulness of DCE-MRI as an assessment tool for the meningeal lymphatic vessels.

We hypothesized that a distinct dynamic enhancement pattern would be depicted in the PSD, which is thought to harbor meningeal lymphatic vessels and is distinguishable from that of adjacent venous structures. We also hypothesized that dynamic changes in PSD would occur during the aging process. Therefore, this study aimed to investigate the effectiveness of DCE-MRI with an intravenous injection of a gadolinium contrast agent in depicting dynamic patterns of PSD in neurologically normal participants from other venous structures and to evaluate the difference in dynamic contrast enhancement patterns in the PSD between older adults and their younger counterparts.

MATERIALS AND METHODS

This prospective study was approved by the Gangnam Severance Hospital Institutional Review Board (IRB No. 3-2020-0480) and conducted in accordance with the Declaration of Helsinki. Written informed consent was obtained from all the participants.

Study Participants

In this prospective feasibility study, 21 neurologically healthy participants were screened for recruitment between May 2021 and October 2021. Inclusion criteria for participants were as follows: 1) aged ≥ 19 years, 2) no history of neurological or psychiatric disease, 3) intact activities of daily living, 4) Mini-Mental State Examination (MMSE) scores of ≥ 26; and 5) an estimated glomerular filtration rate of ≥ 60 mL/min/1.73 m^2 tested within a year. The exclusion criteria were as follows: 1) significantly abnormal findings or severe artifacts on brain MRI and 2) a physician-indicated contraindication to an MRI examination. One participant was excluded because of a history of allergy to contrast media, and two additional participants were later excluded because of severe motion artifacts in the MRI. Finally, 18 participants were enrolled in this study and were grouped into young participants (< 65 years; n = 9) and older adult participants (≥ 65 years; n = 9). A flowchart of participant inclusion in the study is shown in Figure 1.

Clinical Evaluation

All participant's medical conditions (including a history of hypertension, diabetes, and hyperlipidemia), MMSE, and Clinical Dementia Rating (CDR) scores were assessed.

MRI Protocol

All examinations were conducted using a 3 T scanner (MAGNETOM VIDA, Siemens Healthcare). The image sequences included sagittal three-dimensional (3D) magnetization-prepared rapid acquisition with gradient echo imaging, axial T2-weighted imaging, axial susceptibility-weighted imaging, sagittal 3D T2-weighted FLAIR, coronal DCE-MRI, and sagittal contrast-enhanced 3D T1-weighted black blood imaging (3D T1 BB). The parameters for each sequence are listed in Supplementary Table 1. DCE-MRI was acquired using the golden-angle radial sparse parallel-volumetric interpolated breath-hold (GRASP-VIBE) sequence and consisted of 92 series with time intervals of 6.2 s. Each series was composed of 30 sections of coronal images with

 https://doi.org/10.3348/kjr.2022.0980

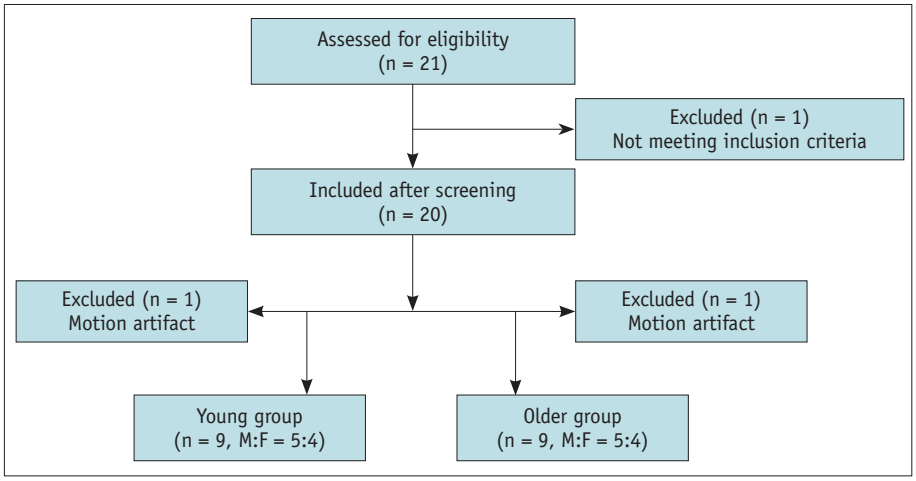

Fig. 1. Flowchart of participant inclusion.

3.0 mm thickness and acquired in an anterior-posterior direction with the level of the corpus callosum genu being the foremost plane. The following imaging parameters were used for DCE-MRI: repetition time, 6.24 ms; echo time, 2.91 ms; field of view, 240 x 240 mm; voxel size, 0.625 x 0.625 x 3.0 mm^3. At the 10th dynamic phase, a gadolinium-based contrast agent was injected (0.2 mL/kg ProHance, Bracco) at a rate of 4 mL/s, followed by 30 mL of saline bolus (Supplementary Fig. 1). The total acquisition time for DCE-MRI was 9 min 32 sec. After DCE-MRI acquisition, contrast-enhanced 3D T1 BB was performed without additional contrast injection.

Imaging Analysis

To investigate the distinct enhancement pattern of the meningeal lymphatic vessels, three circular regions of interests (ROIs) were manually placed by a neuroradiologist with 9 years of experience in neuroradiology, with reference to the contrast-enhanced 3D T1 BB and 3D T2 FLAIR images in the following areas: PSD, SSS, and cortical vein (CV; Fig. 2). PSD was defined as the area along the middle to posterior segment of the SSS showing intermediate or high signals on 3D T1 BB (not vascular structures) and signals not suppressed on 3D T2 FLAIR images (not CSF space) [12]. The ROI on the PSD was placed at the superolateral aspect of the SSS, which is known to harbor meningeal lymphatic vessels [6-8,12]. The ROI size ranges for PSD, SSS, and CV were 0.39–5.08 mm^2, 0.78–15.62 mm^2, and 0.39–5.86 mm^2, respectively.

For each ROI, DCE-MRI results were automatically analyzed qualitatively and semi-quantitatively using time-intensity curve analysis in the Olea Sphere 2.2 software (Olea Medical). For qualitative analysis, the enhancement phase was divided into early and delayed phases based on 2 min post-contrast agent injection [17]. The enhancement pattern of the early phase was then classified based on the percentage increase in signal intensity from the precontrast levels, with increases of < 50%, 50%–100%, and > 100% considered as slow, medium, and fast, respectively. The enhancement pattern of the delayed phase was classified as persistent (defined as a continuous increase in the enhancement of > 10% early enhancement), plateau (constant signal intensity once the peak reaches ±10% early enhancement), and wash-out (decreasing signal intensity after peak enhancement of > 10% early enhancement) [18].

For semi-quantitative analysis, the following six kinetic curve-derived parameters were obtained: wash-in rate; wash-out rate; peak enhancement ratio, defined as (maximum signal intensity – precontrast signal intensity [PER])/PER; time to peak enhancement (TTP); relative wash-out, defined as (maximum signal intensity – end signal intensity)/(maximum signal intensity – PER), and area under the curve (AUC) [19,20].

To measure the maximal thickness of the PSD, sagittal contrast-enhanced 3D T1 BB images were reformatted into coronal and axial 1 mm slices. We noted the presence of hyperintense signals around the SSS; based on methods detailed in a previous study [21], an experienced neuroradiologist measured its maximum thickness on the coronal images of the anterior, middle, and posterior sagittal sinus, perpendicular to the posterolateral wall of the PSD to the SSS.

For the analysis of inter-rater reliability, another neuroradiologist with 4 years of experience in neuroradiology independently placed ROIs in the PSD, and kinetic curve-

https://doi.org/10.3348/kjr.2022.0980

Korean Journal of Radiology
KJR

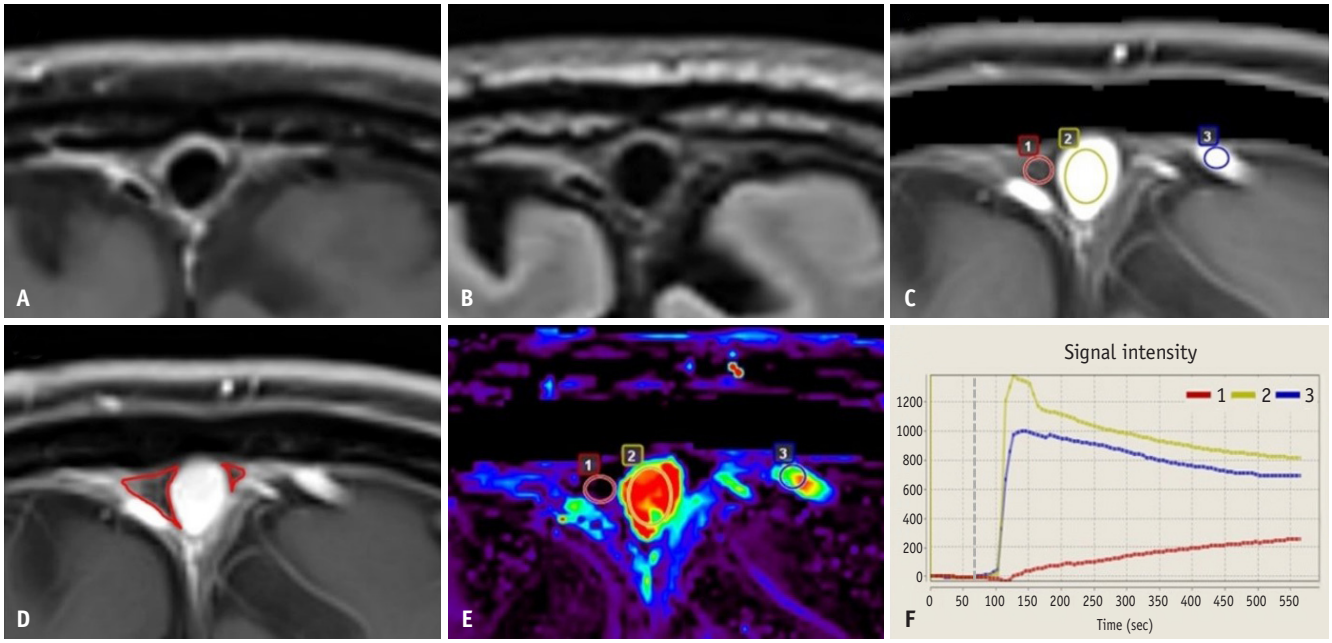

Fig. 2. An example of regions of interest (ROI) placement. An example of ROI placement around the posterior superior sagittal sinus (SSS) is shown in the images of a 71-year-old male participant. Referencing the contrast-enhanced 3D T1 BB **(A)** and 3D T2 FLAIR **(B)** images, three circular ROIs were manually placed on the dynamic contrast-enhanced magnetic resonance imaging (DCE-MRI) images **(C)** by an experienced neuroradiologist. The red, yellow, and blue circles represent ROIs placed on the parasagittal dural space (PSD), SSS, and cortical vein, respectively. **D:** The PSD is depicted as the area at the superolateral aspect of the SSS outlined by red lines on a late-phase DCE-MRI image. After these three ROIs were transferred to the processed DCE-MRI maps (an example of the peak enhancement ratio map is depicted) **(E)**, the final time-intensity curve for each ROI was generated **(F)**. The timing of the contrast injection is indicated by the gray dashed line. 3D T1 BB = three-dimensional T1-weighted black blood imaging, 3D T2 FLAIR = three-dimensional T2 fluid-attenuated inversion recovery imaging

derived parameters were obtained for all participants.

Statistical Analysis

Categorical data are shown as the number of observations (percentage), and continuous data are shown as the median (interquartile range [IQR]), according to normality tests using the Kolmogorov-Smirnov test. Demographic and clinical characteristics were compared between the young and older adult participants using the Mann–Whitney U test or Fisher's exact test.

Intraclass correlation coefficients (ICC) were obtained using a two-way random model and an absolute agreement type for each parameter to assess inter-rater reliability. ICC estimate values of < 0.5, 0.5–0.75, 0.75–0.9, and > 0.90 were indicative of poor, moderate, good, and excellent reliability, respectively [22].

Enhancement patterns in the early and delayed phases were dichotomized into non-fast versus fast patterns and non-wash-out versus wash-out patterns, respectively. Comparisons of the dichotomized enhancement patterns of the early and delayed phases in the three ROIs (PSD, SSS, and CV) were analyzed using the chi-square test. The kinetic curve-derived parameters of each ROI were compared using the Kruskal-Wallis test with post-hoc Bonferroni corrections.

We investigated the differences in the enhancement patterns or the kinetic curve-derived parameters of the three ROIs (PSD, SSS, and CV) between the young and older adult participants using Fisher's exact test for pattern comparison and Mann–Whitney U test for kinetic curve-derived parameter comparison. To compare the maximal thickness of the anterior, middle, and posterior PSD between young and older adult participants, the Mann–Whitney U test was performed for each area. Statistical analyses were performed using SPSS (version 25.0; IBM Corporation) and MedCalc (version 9.3.6.0; MedCalc Software). Statistical significance was set at a two-tailed level of 0.05.

RESULTS

Participant Characteristics

The participants' demographic and clinical characteristics are summarized in Table 1. The younger participants were

 https://doi.org/10.3348/kjr.2022.0980

significantly younger than the older adult participants (median 28.0 [IQR 26.8–35.3] years vs. 66.5 [IQR 65.8–69.5] years; $P < 0.001$). The MMSE score was significantly higher in young participants than in older adult participants (median 30.0 [IQR 29.8–30.0] vs. 28.5 [IQR 28.0–30.0]; $P = 0.040$]. There were no significant differences between the two groups in several factors including: sex; CDR score; and the presence of hypertension, diabetes, and hyperlipidemia.

Inter-Rater Reliability of Kinetic Curve-Derived Parameters of PSD

ICC analysis showed moderate or good inter-rater reliability for the following kinetic curve-derived parameters of the PSD: wash-in rate, 0.700 (95% confidence interval [CI], 0.209–0.887); wash-out rate, 0.769 (95% CI, 0.389–0.913); PER, 0.683 (95% CI, 0.150–0.881); TTP, 0.697 (95% CI, 0.197–0.887); relative wash-out, 0.755 (95% CI, 0.364–0.907); and AUC, 0.605 (95% CI, 0.023–0.848).

Table 1. Participant Characteristics

Characteristic	Young Adults (n = 9)	Older Adults (n = 9)	*P*
Age, yr	28.0 (26.8–35.3)	66.5 (65.8–69.5)	< 0.001
Sex (M:F)	5:4	5:4	1.000
MMSE score	30.0 (29.8–30.0)	28.5 (28.0–30.0)	0.040
CDR score	0 (0–0)	0 (0–0)	1.000
Hypertension	0 (0)	4 (44.4)	0.082
Diabetes	1 (11.1)	2 (22.2)	1.000
Hyperlipidemia	0 (0)	3 (33.3)	0.206

Data are median (interquartile range) or number of patients with percentage in parentheses. CDR = Clinical Dementia Rating, F = female, M = male, MMSE = Mini-Mental State Examination

Comparisons of Dynamic Enhancement among PSD, SSS, and CV

In the early phase, two (11.1%) of the 18 participants showed fast enhancement patterns in the PSD. Among the 18 participants, a fast enhancement pattern was observed in the SSS of all (100%) participants and CV of 16 (88.9%) participants ($P < 0.001$). In the delayed phase, a wash-out pattern was only observed in four (22.2%) PSDs of 18 participants; whereas a wash-out pattern was observed in all (100%) SSSs and 17 (94.4%) CVs ($P < 0.001$) (Table 2).

All six kinetic curve-derived parameters, including wash-in rate, wash-out rate, PER, TTP, relative wash-out, and AUC, differed significantly among the three ROIs (all $P < 0.001$). In the post-hoc analysis with Bonferroni corrections, PSD showed distinct values than the other two structures (Table 3).

Age-Associated Differences in the Dynamic Enhancement of PSD

In the early phase, no participants in the older adult group demonstrated a fast enhancement pattern (n = 0, 0%),

Table 2. Enhancement Pattern Comparisons among PSD, SSS, and CV

Phase	Enhancement Pattern	PSD (n = 18)	SSS (n = 18)	CV (n = 18)	*P*
Early	Slow or medium	16 (88.9)	0 (0)	2 (11.1)	< 0.001
	Fast	2 (11.1)	18 (100)	16 (88.9)	
Delayed	Persistent or plateau	14 (77.8)	0 (0)	1 (5.6)	< 0.001
	Wash-out	4 (22.2)	18 (100)	17 (94.4)	

Data are number of patients with percentage in parentheses. CV = cortical vein, PSD = parasagittal dural space, SSS = superior sagittal sinus

Table 3. Kinetic Curve-Derived Parameter Comparison among PSD, SSS, and CV

Parameter	PSD (n = 18)	SSS (n = 18)	CV (n = 18)	*P*	Bonferroni-Corrected *P*		
					PSD vs. SSS	PSD vs. CV	SSS vs. CV
Wash-in rate	1.37 (0.72–4.34)	8.54 (7.86–9.19)	8.05 (6.75–8.93)	< 0.001	< 0.001	< 0.001	1.000
Wash-out rate	0.13 (0.04–0.32)	0.82 (0.70–0.95)	0.70 (0.54–0.80)	< 0.001	< 0.001	< 0.001	0.471
Peak enhancement ratio	241.81 (165.37–330.34)	886.43 (818.68–934.84)	843.57 (692.60–920.15)	< 0.001	< 0.001	< 0.001	0.784
Time to peak, sec	244.62 (158.10–531.65)	121.16 (116.23–127.31)	139.63 (127.31–164.25)	< 0.001	< 0.001	0.022	0.008
Relative wash-out	0.34 (-7.98–19.03)	-29.54 (-31.64 – -27.49	-24.50 (-29.15 – -15.38)	< 0.001	< 0.001	0.006	0.270
AUC	90301.69 (60049.86–117905.43)	305449.41 (260017.86–324063.35)	300425.44 (267929.56–350166.00)	< 0.001	< 0.001	< 0.001	1.000

Kinetic curve-derived parameters are presented as medians and interquartile ranges. AUC = area under the curve, CV = cortical vein, PSD = parasagittal dural space, SSS = superior sagittal sinus

https://doi.org/10.3348/kjr.2022.0980

Korean Journal of Radiology
KJR

whereas two participants in the young participant group demonstrated a fast enhancement pattern (n = 2, 22.2%); however, this difference was not significant (P = 0.470). In the delayed phase, there was only one participant who showed a wash-out pattern in the older adult group (n = 1, 11.1%), whereas three participants showed wash-out patterns in the young group (n = 3, 33.3%); however, this difference was not significant (P = 0.576) (Table 4).

Concerning the kinetic curve-derived parameters, the median wash-out rate in the young participant group (0.32, IQR 0.07–0.45) was significantly higher than that in the older adult participant group (0.09, IQR 0.01–0.15; P = 0.04). However, no significant differences were found in the other five kinetic curve-derived parameters between the two groups (Table 5, Fig. 3). In addition, no significant differences were found in any of the kinetic curve-derived parameters for SSS and CV between the two groups (Supplementary Table 2). Representative time-intensity curves for young and older adult participants are shown in Figure 4.

Age-Associated Differences in the PSD Maximal Thickness

The older adult participants had a higher median thickness of anterior (4.4 mm [IQR 3.2–5.1] vs. 3.2 mm [IQR 2.2–3.6]; P = 0.008), middle (5.9 mm [IQR 5.0–7.8] vs. 4.4 mm [IQR 3.5–5.0]; P = 0.031), and posterior (6.7 mm [IQR 6.6–7.0] vs. 2.8 mm [IQR 2.7–3.3]; P < 0.001) PSD.

Table 4. Comparison of Enhancement Patterns in the Parasagittal Dural Space between Young and Older Adult Participants

Phase	Enhancement Pattern	Young Adults (n = 9)	Older Adults (n = 9)	*P*
Early	Slow or medium	7 (77.8)	9 (100)	0.470
	Fast	2 (22.2)	0 (0)	
Delayed	Persistent or plateau	6 (66.7)	8 (88.9)	0.576
	Wash-out	3 (33.3)	1 (11.1)	

Data are number of patients with percentage in parentheses

DISCUSSION

This study investigated in vivo dynamic assessment of meningeal lymphatic vessels in neurologically normal young and older participants using DCE-MRI. Meningeal lymphatic enhancement in the PSD around the SSS showed a distinct dynamic enhancement pattern from adjacent venous structures, confirming that PSD is not a constituent of the venous system but of the meningeal lymphatic system itself, as previously suggested [6,12]. Furthermore, on semi-quantitative analysis, delayed wash-out of PSD was found in older adult participants than in young participants, which may represent meningeal lymphatic stasis and, consequently, meningeal lymphatic drainage dysfunction.

Recently, both animal and human studies reported the presence of a lymphatic system within the meninges [3-8,11-13,15,16,21,23-25]. However, most prior in vivo studies have either assessed only the morphological features of meningeal lymphatic vessels [21,26] or required the invasive off-label use of a gadolinium agent with a very long scan time of > 24 h, which may limit its wider clinical application [11-14]. Only a few studies have utilized intravenous injection of a contrast agent to assess the function of the meningeal lymphatic system. A recent study reported that meningeal lymphatic vessels around the SSS showed distinct enhancement on T1 BB or T2 FLAIR images after intravenous injection of gadolinium contrast in healthy participants [6]. Another study applied DCE-MRI with an intravenous injection of gadolinium contrast in patients with various Parkinsonian disorders and reported that the disease diagnosis could affect meningeal lymphatic drainage differently [16]. The main strength of our study is that it provides an easily applicable method that can be performed within an acceptable scan time in daily practice. Moreover, since meningeal lymphatic dysfunction has been

Table 5. A Kinetic Curve-Derived Parameter Comparison of the Parasagittal Dural Space between Young and Older Adult Participants

Parameter	Young Adults (n = 9)	Older Adults (n = 9)	*P*
Wash-in rate	0.73 (0.26–4.62)	1.72 (0.80–4.36)	0.489
Wash-out rate	0.32 (0.07–0.45)	0.09 (0.01–0.15)	0.040
Peak enhancement ratio	76.0 (31.6–117.9)	61.8 (31.7–90.4)	0.546
Time to peak, sec	364.4 (145.8–535.8)	224.3 (167.3–518.3)	1.000
Relative wash-out	-5.0 (-21.4–17.5)	4.8 (-7.7–37.8)	0.387
Area under the curve	94905.7 (40005.9–123849.6)	85697.7 (61601.3–114861.3)	1.000

Kinetic curve-derived parameters are presented as medians and interquartile ranges

https://doi.org/10.3348/kjr.2022.0980

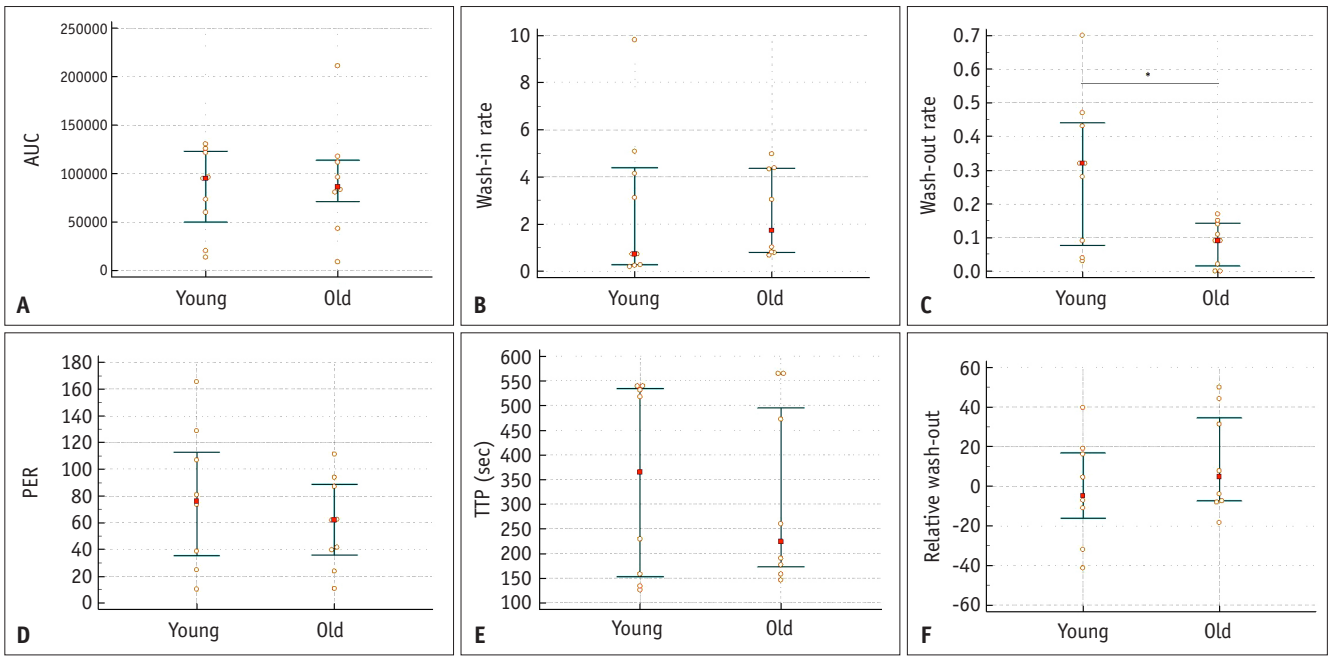

Fig. 3. Comparisons of kinetic curve-derived parameters in parasagittal dural space between young and older adult participants. **(A-F)** The central red dots and whiskers represent the medians and interquartile ranges, respectively. *Statistically significant difference. AUC = area under the curve, PER = peak enhancement ratio, TTP = time-to-peak enhancement

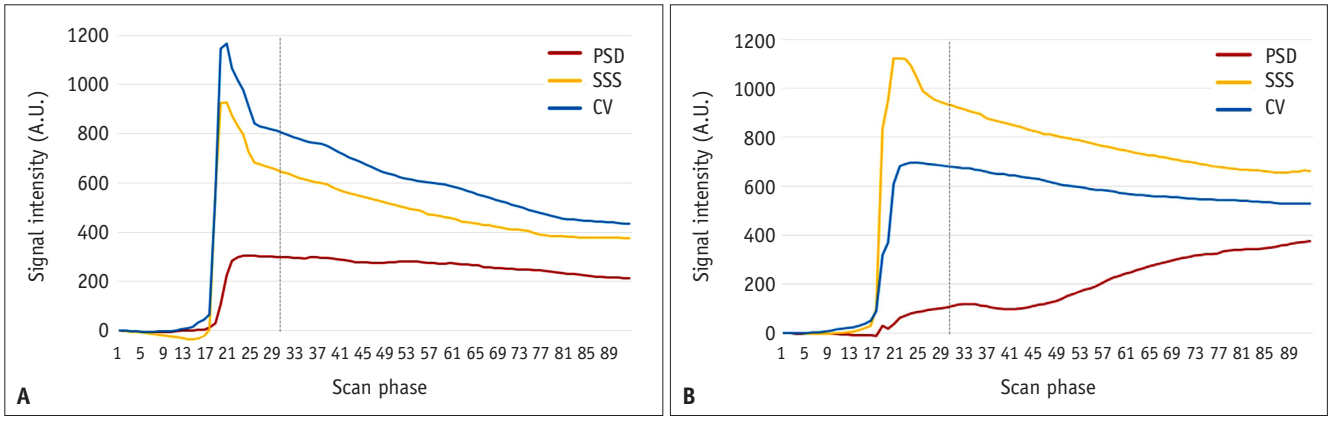

Fig. 4. Representative time-intensity curves of young **(A)** and older adult **(B)** participants. The dashed lines representing 2 min after contrast injection, divide the early and delayed phases. CV = cortical vein, PSD = parasagittal dural space, SSS = superior sagittal sinus, A.U. = arbitrary units

proposed as an aggravating factor in Alzheimer's disease pathology and age-associated cognitive decline [23], this in vivo monitoring tool using DCE-MRI may serve as a valuable imaging biomarker for assessing the functional capability of meningeal lymphatics.

Initially, the enhancing structure visible adjacent to the major intracranial venous sinuses on MRI had, been considered as a meningeal lymphatic vessel itself [6]; however, rather than being the meningeal lymphatic vessel itself, this has now been considered to be the parasinus dural space which consists of prominent intradural channels that are supposed to work as a barrier for CSF drainage into the venous or lymphatic systems [12,27-30]. Considering the absence of blood-meningeal barriers in dural blood vessels, the enhancement detected in PSD after intravenous injection of gadolinium agent may reflect that the gadolinium contrast agent in the dura mater migrates to collecting lymphatics in PSD, through which it finally drains into the extracranial cervical lymph nodes [8,15,16]. Given that PSD harbors meningeal lymphatic vessels [23,31], it appears reasonable to suggest that our DCE-MRI technique, which focuses on PSD, is a practical method for the

https://doi.org/10.3348/kjr.2022.0980

Korean Journal of Radiology
KJR

assessment of meningeal lymphatic drainage.

Previous animal studies have highlighted decreased meningeal lymphatic function in addition to different genetic expressions in the endothelial cells of meningeal lymphatic vessels in aged mice, which may explain age-associated cognitive decline or neurological conditions [23,32]. A recent human MRI study also reported meningeal lymphatic dysfunction in older adult participants using intrathecal gadolinium injection, which exhibited delayed clearance of meningeal lymphatic vessels in this population [11]. Additionally, researchers have described morphological changes in the PSD in relation to aging and reported an age-related increase in the volume/thickness of the PSD [21,26,33]. These findings of age-related functional and morphologic changes in the PSD are consistent with our observation that older adult participants had increased PSD thickness and delayed PSD contrast wash-out compared to that of younger participants, which may represent meningeal lymphatic system stasis. Furthermore, these findings seem to be consistent with general age-related dilatation and contractile dysfunction of lymphatic vessels [34,35].

This feasibility study had some limitations. First, only a small number of participants were enrolled. Further studies with a larger number of subjects are needed to implement DCE-MRI as a tool to evaluate the meningeal lymphatic system in clinical practice. Second, all participants were neurologically healthy individuals. Although the aging process is known to cause meningeal lymphatic dysfunction, participants with various diseases that may induce meningeal lymphatic dysfunction, such as Alzheimer's disease or traumatic brain injury, may show clearer differences in the dynamic changes in the PSD. Third, some participants had vascular risk factors such as hypertension, diabetes, and hyperlipidemia, which have been proven by both animal and human studies to be associated with glymphatic dysfunction [36-40]. However, to date, these vascular risk factors have not been proven to have an effect on meningeal lymphatic function. Nevertheless, these common vascular risk factors may potentially affect meningeal lymphatic function and the glymphatic system. Further investigations are required to address this issue. Fourth, although there was moderate to good inter-rater reliability for dynamic parameters showing ICC values > 0.6 in all parameters, the manual placement of ROIs on a small structure may lead to possible reproducibility issues. To address this issue, we plan to automate the positioning of the ROI on the PSD using an artificial intelligence-based approach. Finally, test-retest reliability was not evaluated in this study. Future studies should address this issue to validate the applicability of DCE-MRI in the evaluation of meningeal lymphatic function.

In conclusion, the findings of this feasibility study demonstrated the in vivo dynamic nature of the meningeal lymphatic system in PSD using DCE-MRI with intravenous injection of a contrast agent, which is different from that of adjacent venous structures. Delayed wash-out was more pronounced in the PSD of older adult participants, suggesting that the aging process may disturb meningeal lymphatic drainage. Future studies that include patients with various neurological diseases are warranted to determine whether this quantitative DCE-MRI technique can facilitate the assessment of diseases and the associated dysfunction of the meningeal lymphatics.

Supplement

The Supplement is available with this article at https://doi.org/10.3348/kjr.2022.0980.

Availability of Data and Material

The datasets generated or analyzed during the study are available from the corresponding author on reasonable request.

Conflicts of Interest

Sang Hyun Suh, a contributing editor of the *Korean Journal of Radiology*, was not involved in the editorial evaluation or decision to publish this article. All remaining authors have declared no conflicts of interest.

Author Contributions

Conceptualization: Mina Park. Data curation: Bio Joo, Sung Jun Ahn. Formal analysis: Bio Joo. Funding acquisition: Mina Park. Investigation: Mina Park. Methodology: Mina Park. Resources: Mina Park. Software: Sung Jun Ahn. Supervision: Sang Hyun Suh. Validation: Mina Park. Visualization: Bio Joo. Writing—original draft: Bio Joo. Writing—review & editing: Mina Park.

ORCID iDs

Bio Joo
https://orcid.org/0000-0001-7460-1421
Mina Park
https://orcid.org/0000-0002-2005-7560
Sung Jun Ahn
https://orcid.org/0000-0003-0075-2432

Sang Hyun Suh
https://orcid.org/0000-0002-7098-4901

Funding Statement

This study was supported by a faculty research grant of Yonsei University College of Medicine (6-2019-0098) and by the National Research Foundation of Korea (NRF) grant funded by the Korea government (MSIT) (No. NRF-2020R1C1C1005724).

Acknowledgments

We would like to thank In-seong Kim, PhD of Siemens Korea for his contribution in the protocol setting.

REFERENCES

1. Galea I, Bechmann I, Perry VH. What is immune privilege (not)? *Trends Immunol* 2007;28:12-18
2. Carson MJ, Doose JM, Melchior B, Schmid CD, Ploix CC. CNS immune privilege: hiding in plain sight. *Immunol Rev* 2006;213:48-65
3. Aspelund A, Antila S, Proulx ST, Karlsen TV, Karaman S, Detmar M, et al. A dural lymphatic vascular system that drains brain interstitial fluid and macromolecules. *J Exp Med* 2015;212:991-999
4. Louveau A, Smirnov I, Keyes TJ, Eccles JD, Rouhani SJ, Peske JD, et al. Structural and functional features of central nervous system lymphatic vessels. *Nature* 2015;523:337-341
5. Ahn JH, Cho H, Kim JH, Kim SH, Ham JS, Park I, et al. Meningeal lymphatic vessels at the skull base drain cerebrospinal fluid. *Nature* 2019;572:62-66
6. Absinta M, Ha SK, Nair G, Sati P, Luciano NJ, Palisoc M, et al. Human and nonhuman primate meninges harbor lymphatic vessels that can be visualized noninvasively by MRI. *Elife* 2017;6:e29738
7. Visanji NP, Lang AE, Munoz DG. Lymphatic vasculature in human dural superior sagittal sinus: implications for neurodegenerative proteinopathies. *Neurosci Lett* 2018;665:18-21
8. Goodman JR, Adham ZO, Woltjer RL, Lund AW, Iliff JJ. Characterization of dural sinus-associated lymphatic vasculature in human Alzheimer's dementia subjects. *Brain Behav Immun* 2018;73:34-40
9. Louveau A, Plog BA, Antila S, Alitalo K, Nedergaard M, Kipnis J. Understanding the functions and relationships of the glymphatic system and meningeal lymphatics. *J Clin Invest* 2017;127:3210-3219
10. Hu J, Shen Y, Fahmy LM, Krishnamurthy S, Li J, Zhang L, et al. The role of the parenchymal vascular system in cerebrospinal fluid tracer clearance. *Eur Radiol* 2023;33:656-665
11. Zhou Y, Cai J, Zhang W, Gong X, Yan S, Zhang K, et al. Impairment of the glymphatic pathway and putative meningeal lymphatic vessels in the aging human. *Ann Neurol* 2020;87:357-369
12. Ringstad G, Eide PK. Cerebrospinal fluid tracer efflux to parasagittal dura in humans. *Nat Commun* 2020;11:354
13. Eide PK, Ringstad G. Cerebrospinal fluid egress to human parasagittal dura and the impact of sleep deprivation. *Brain Res* 2021;1772:147669
14. Halvorsen M, Edeklev CS, Fraser-Green J, Løvland G, Vatnehol SAS, Gjertsen Ø, et al. Off-label intrathecal use of gadobutrol: safety study and comparison of administration protocols. *Neuroradiology* 2021;63:51-61
15. Filippopulos FM, Fischer TD, Seelos K, Dunker K, Belanovic B, Crispin A, et al. Semiquantitative 3T brain magnetic resonance imaging for dynamic visualization of the glymphatic-lymphatic fluid transport system in humans: a pilot study. *Invest Radiol* 2022;57:544-551
16. Ding XB, Wang XX, Xia DH, Liu H, Tian HY, Fu Y, et al. Impaired meningeal lymphatic drainage in patients with idiopathic Parkinson's disease. *Nat Med* 2021;27:411-418
17. Petralia G, Summers PE, Agostini A, Ambrosini R, Cianci R, Cristel G, et al. Dynamic contrast-enhanced MRI in oncology: how we do it. *Radiol Med* 2020;125:1288-1300
18. Rahbar H, Partridge SC. Multiparametric MR imaging of breast cancer. *Magn Reson Imaging Clin N Am* 2016;24:223-238
19. Sung YS, Park B, Choi Y, Lim HS, Woo DC, Kim KW, et al. Dynamic contrast-enhanced MRI for oncology drug development. *J Magn Reson Imagin* 2016;44:251-264
20. Gaddikeri S, Gaddikeri RS, Tailor T, Anzai Y. Dynamic contrast-enhanced MR imaging in head and neck cancer: techniques and clinical applications. *AJNR Am J Neuroradiol* 2016;37:588-595
21. Albayram MS, Smith G, Tufan F, Tuna IS, Bostancıklıoğlu M, Zile M, et al. Non-invasive MR imaging of human brain lymphatic networks with connections to cervical lymph nodes. *Nat Commun* 2022;13:203
22. Koo TK, Li MY. A guideline of selecting and reporting intraclass correlation coefficients for reliability research. *J Chiropr Med* 2016;15:155-163
23. Da Mesquita S, Louveau A, Vaccari A, Smirnov I, Cornelison RC, Kingsmore KM, et al. Functional aspects of meningeal lymphatics in ageing and Alzheimer's disease. *Nature* 2018;560:185-191
24. Dai W, Yang M, Xia P, Xiao C, Huang S, Zhang Z, et al. A functional role of meningeal lymphatics in sex difference of stress susceptibility in mice. *Nat Commun* 2022;13:4825
25. Jacob L, de Brito Neto J, Lenck S, Corcy C, Benbelkacem F, Geraldo LH, et al. Conserved meningeal lymphatic drainage circuits in mice and humans. *J Exp Med* 2022;219:e20220035
26. Park M, Kim JW, Ahn SJ, Cha YJ, Suh SH. Aging is positively associated with peri-sinus lymphatic space volume: assessment using 3T black-blood MRI. *J Clin Med* 2020;9:3353
27. Mack J, Squier W, Eastman JT. Anatomy and development of the meninges: implications for subdural collections and CSF circulation. *Pediatr Radiol* 2009;39:200-210
28. Han H, Tao W, Zhang M. The dural entrance of cerebral bridging veins into the superior sagittal sinus: an anatomical comparison between cadavers and digital subtraction

angiography. *Neuroradiology* 2007;49:169-175
29. Fox RJ, Walji AH, Mielke B, Petruk KC, Aronyk KE. Anatomic details of intradural channels in the parasagittal dura: a possible pathway for flow of cerebrospinal fluid. *Neurosurgery* 1996;39:84-90; discussion 90-91
30. Park M, Park JP, Kim SH, Cha YJ. Evaluation of dural channels in the human parasagittal dural space and dura mater. *Ann Anat* 2022;244:151974
31. Da Mesquita S, Fu Z, Kipnis J. The meningeal lymphatic system: a new player in neurophysiology. *Neuron* 2018;100:375-388
32. Ma Q, Ineichen BV, Detmar M, Proulx ST. Outflow of cerebrospinal fluid is predominantly through lymphatic vessels and is reduced in aged mice. *Nat Commun* 2017;8:1434
33. Hett K, McKnight CD, Eisma JJ, Elenberger J, Lindsey JS, Considine CM, et al. Parasagittal dural space and cerebrospinal fluid (CSF) flow across the lifespan in healthy adults. *Fluids Barriers CNS* 2022;19:24
34. Shang T, Liang J, Kapron CM, Liu J. Pathophysiology of aged lymphatic vessels. *Aging (Albany NY)* 2019;11:6602-6613
35. Zolla V, Nizamutdinova IT, Scharf B, Clement CC, Maejima D, Akl T, et al. Aging-related anatomical and biochemical changes in lymphatic collectors impair lymph transport, fluid homeostasis, and pathogen clearance. *Aging Cell* 2015;14:582-594
36. Verheggen ICM, Van Boxtel MPJ, Verhey FRJ, Jansen JFA, Backes WH. Interaction between blood-brain barrier and glymphatic system in solute clearance. *Neurosci Biobehav Rev* 2018;90:26-33
37. Mortensen KN, Sanggaard S, Mestre H, Lee H, Kostrikov S, Xavier ALR, et al. Impaired glymphatic transport in spontaneously hypertensive rats. *J Neurosci* 2019;39:6365-6377
38. Tian Y, Zhao M, Chen Y, Yang M, Wang Y. The underlying role of the glymphatic system and meningeal lymphatic vessels in cerebral small vessel disease. *Biomolecules* 2022;12:748
39. Kikuta J, Kamagata K, Takabayashi K, Taoka T, Yokota H, Andica C, et al. An investigation of water diffusivity changes along the perivascular space in elderly subjects with hypertension. *AJNR Am J Neuroradiol* 2022;43:48-55
40. Zhang Y, Zhang R, Ye Y, Wang S, Jiaerken Y, Hong H, et al. The influence of demographics and vascular risk factors on glymphatic function measured by diffusion along perivascular space. *Front Aging Neurosci* 2021;13:693787